

Rechargeable lithium battery using non-flammable electrolyte basing on tetraethylene glycol dimethyl ether and olivine cathodes

Daniele Di Lecce^a, Lorenzo Carbone^a, Vincenzo Gancitano^b, Jusef Hassoun^{b,*}

^a Chemistry Department, Sapienza University of Rome, Piazzale Aldo Moro, 5, 00185, Rome, Italy

^b Department of Chemical and Pharmaceutical Sciences, University of Ferrara, Via Fossato di Mortara, 17, 44121, Ferrara, Italy

* Corresponding author: jusef.hassoun@unife.it

Highlights

- Tetraethylene glycol dimethyl ether electrolyte is used in lithium metal cells
- The TEGDME electrolyte is not flammable
- LiFePO_4 and $\text{LiMn}_{0.5}\text{Fe}_{0.5}\text{PO}_4$ olivines are used as the cathodes
- The electrode powders have homogenous morphology and composition
- The cells exhibit suitable performances

Keywords

Tetraethylene glycol dimethyl ether; non-flammable electrolyte; lithium metal; LiFePO_4 ;
 $\text{LiMn}_{0.5}\text{Fe}_{0.5}\text{PO}_4$

Abstract

We propose lithium metal cells employing LiCF_3SO_3 -tetraethylene glycol dimethyl ether (TEGDME) electrolyte solution with LiFePO_4 and $\text{LiMn}_{0.5}\text{Fe}_{0.5}\text{PO}_4$ cathodes. The electrolyte is selected due to its non-flammability, herein demonstrated, and considered as a key requirement for application cells employing high energy lithium metal anode. The selected olivine cathodes, i.e., stable materials prepared by solvothermal pathway, have regular submicrometric morphology suitable for cell operation and homogeneous composition, as confirmed by electron microscopy and energy dispersive X-ray

spectroscopy. The electrochemical tests reveal promising cycling performances in terms of delivered capacity, stability and rate capability. The Li/LiCF₃SO₃-TEGDME/LiFePO₄ cell operates at 3.5 V with capacity ranging from 150 mAh g⁻¹ at C/10 to 110 mAh g⁻¹ at 2C, while the Li/LiCF₃SO₃-TEGDME/LiFe_{0.5}Mn_{0.5}PO₄ cell performs following two plateaus at 4.1 V and 3.5 V with capacity ranging from 160 mAh g⁻¹ at C/10 to 75 mAh g⁻¹ at 2C. Hence, the results demonstrate the suitability of TEGDME-based electrolytes in combination with LiFePO₄ and LiFe_{0.5}Mn_{0.5}PO₄ cathodes for high performances lithium metal battery.

Introduction

Most of the recent developments in energy storage technology have been focused on Li-ion battery, involving improvements of chemistry and composition of the electrode materials [1], being the LiPF₆-alkyl carbonate solution the principal choice for the electrolyte [2]. Therefore, the present Li-ion technology, employing a transition metal compound-based cathode and a carbon-based anode, allows reversible energy storage with mitigation of the drawbacks related to the use of metallic lithium [3]. Cells exploiting lithium metal are generally limited to primary, non-rechargeable configuration, due to possible dendrite formation throughout lithium deposition/stripping at anode side, which may lead to internal short circuit and associated risks upon prolonged cycling in flammable organic electrolytes [4–6]. Nevertheless, metallic lithium has ideal theoretical features, such as high theoretical specific capacity (3860 mAh g⁻¹), low density (0.59 g cm⁻³), and the lowest electrochemical potential (–3.040 V vs. the standard hydrogen electrode) [4]. Rechargeable lithium metal batteries have been proposed by exploiting electrolytes of relevant safety, such as those basing on polymer or solid state configurations [4]. Among them, polyethylene oxide (PEO) [7], and glass type (LISICON, NASICON) [8] electrolytes represent the most suitable media. Hence, an effective approach to increase safety level and reliability of rechargeable cells employing lithium metal anode may be the use of stable and non-flammable electrolyte solutions.

Poly(ethylene glycol)dialkyl ethers (i.e., $R_1O(CH_2CH_2O)_nR_2$), known as end-capped glymes, are characterized by a high flash point and suitable features as aprotic solvents for lithium salts [9]. However, glyme-based electrolytes have revealed poor electrode passivation properties, which limit their application in rechargeable Li-battery due to continuous solvent decomposition by cell operation [10,11]. This issue has been mitigated by using film forming additives, e.g., lithium nitrate ($LiNO_3$), which improve the passivating film on the electrode surface [12–14]. Hence, electrolyte solutions based on glymes have been extensively studied in Li-S [15–19] and Li-O₂ batteries [20–24], while only few papers reported application with insertion cathodes [25–27]. In particular, a previous work demonstrated that $LiNO_3$ addition to a glyme-based electrolyte solution leads to stable solid electrolyte interface (SEI) formation over the electrode surface, thus allowing proper operation of a lithium cell employing $LiFePO_4$ cathode [27]. Olivine materials based on Fe and Mn are characterized by remarkable stability of the polyanionic framework [28,29] and have working voltage below 4.5 V vs. Li^+/Li [30,31], i.e., suitable features for application in cells using lithium metal anode and ether-based electrolyte [18]. Therefore, the electrochemical study of $LiFe_{1-\alpha}Mn_{\alpha}PO_4$ olivines in glyme-based solutions is expected to effectively contribute to the development of rechargeable lithium cells.

Several synthetic approaches have been studied in order to achieve olivine cathodes with controlled morphology and proper particle size for ensuring efficient electrochemical process with limited electrolyte decomposition [32–39]. The use of alternative electrolytes designed for lithium metal cell, such as those basing on end-capped glyme solvents, may lead to a narrow voltage window with respect to conventional carbonate-based solutions [27]. This choice reasonably requires further careful morphology optimization of the $LiFe_{1-\alpha}Mn_{\alpha}PO_4$ cathode. Indeed the particle size plays a crucial role for allowing fast Li^+ insertion/deinsertion at the high rates and contemporary ensures limited parasitic processes at low current [40,41].

Accordingly, we employ morphologically optimized LiFePO_4 and $\text{LiMn}_{0.5}\text{Fe}_{0.5}\text{PO}_4$ olivine materials [42] in lithium metal cells using a solution of lithium triflate (LiCF_3SO_3) in tetraethylene glycol dimethyl ether (TEGDME) as electrolyte. This particular electrolyte formulation has already shown suitable characteristics in terms of thermal properties, lithium ion conductivity, and electrochemical stability window [18]. Additional, *ad hoc* designed test demonstrate herein a complete non-flammability of this promising electrolyte. The morphology and atomic composition of the olivine cathodes are studied by scanning electron microscopy (SEM), transmission electron microscopy (TEM), and energy-dispersive X-ray spectroscopy (EDS). Hence, the electrochemical performances of the $\text{Li}/\text{LiCF}_3\text{SO}_3\text{-TEGDME}/\text{LiFe}_{1-\alpha}\text{Mn}_\alpha\text{PO}_4$ ($\alpha = 0, 0.5$) cells are evaluated by galvanostatic cycling at several current rates. To the best of our knowledge, the results herein reported demonstrate for the first time the applicability of $\text{LiCF}_3\text{SO}_3\text{-LiNO}_3\text{-TEGDME}$ with LiFePO_4 and $\text{LiMn}_{0.5}\text{Fe}_{0.5}\text{PO}_4$ cathodes and lithium metal anode.

Experimental

C-coated LiFePO_4 and $\text{LiMn}_{0.5}\text{Fe}_{0.5}\text{PO}_4$ powders (C content of about 5 wt. %) with olivine structure were synthesized by using a solvothermal pathway followed by high-temperature annealing in Ar atmosphere as previously reported [29,42]. Sample morphology was investigated by scanning electron microscopy (SEM) and transmission electron microscopy (TEM). SEM images were acquired by using a Zeiss EVO 40 microscope, equipped with a LaB_6 thermo-ionic electron gun. The atomic composition of the samples was studied by SEM-energy dispersive X-ray spectroscopy (EDS), by using a X-ACT, Cambridge Instruments analyzer. TEM images were taken by a Zeiss EM 910 microscope, equipped with a tungsten thermo-ionic electron gun operating at 100 kV. The samples were suspended in water, sonicated, and deposited onto a Formvar[®] support film applied to Cu grid for TEM.

The electrolyte solution was prepared in Ar-filled glovebox by dissolving lithium trifluoromethanesulfonate (lithium triflate, LiCF_3SO_3 , Sigma-Aldrich) and lithium nitrate (LiNO_3 , Sigma-Aldrich) in tetraethylene glycol dimethyl ether (TEGDME, Sigma-Aldrich) solvent; both salts were used in 1 mol kg^{-1} concentration with respect to the solvent. Prior to electrolyte preparation, the salts were dried under vacuum at $100 \text{ }^\circ\text{C}$ for 24 h and TEGDME was dried under molecular sieves. The final water content in TEGDME was below 10 ppm by Karl Fisher titration (831 Karl Fisher Coulometr, Metrohm).

The cathode slurries were prepared by mixing active material (LiFePO_4 , $\text{LiMn}_{0.5}\text{Fe}_{0.5}\text{PO}_4$), poly(vinylidene fluoride-hexafluoropropylene) (PVdF-HFP copolymer, Kynar Flex 2801) binder, and Super P Carbon (Timcal) conductive additive in the ratio 80:10:10% w/w. Tetrahydrofuran (THF, Sigma-Aldrich) was used as solvent for the electrode slurries. The slurries were deposited on carbon-cloth current collector by doctor blade, casted, dried overnight under vacuum at $110 \text{ }^\circ\text{C}$, and cut in the form of 10 mm diameter disks. The electrode mass loading was about 4 mg cm^{-2} . Additional LiFePO_4 electrodes were prepared using Al foil, in order to evaluate the effect of the current collector (see the Supplementary Information). T-type cells were assembled in Ar-filled glovebox by stacking cathode, glass fiber separator (Whatman) soaked in the electrolyte solution (LiCF_3SO_3 - LiNO_3 -TEGDME), and lithium metal anode. Benchmark electrolyte solution, i.e., 1 M LiPF_6 in ethylene carbonate (EC):dimethyl carbonate (DMC) 1:1 w/w, was used for flammability tests and Li/LiFePO₄ reference cells (see the Supplementary Information). The cell case had three stainless steel cylinders as current collectors and polypropylene holder; the cell was sealed by polypropylene screws. The flammability tests were carried out on the electrolytes just taken out from the glovebox.

Rate capability tests on two-electrodes lithium cells were performed by galvanostatic cycling at C/10, C/5, C/3, C/2, 1C, and 2C rates ($1\text{C} = 170 \text{ mAh g}^{-1}$), within the 2 – 4 V and 2 – 4.3 V voltage ranges for LiFePO_4 and $\text{LiMn}_{0.5}\text{Fe}_{0.5}\text{PO}_4$, respectively. Galvanostatic cycling tests using a single current

rate were performed at C/5, C/3, and 2C rates. All the cells using glyme-based electrolyte were activated by 4 galvanostatic cycles at C/5 rate; the first discharge was performed by decreasing the voltage below 2 V and limiting the time to 5.15 h, according to a previously reported procedure [27] suitable for the formation of a stable SEI layer at the electrode surface (see the Supplementary Information). All the cycling tests were carried out at room temperature through a Maccor 4000 series Battery Test System.

Results and discussion

The employment of glyme and olivine electrode may actually hinder the safety issues related to the use of lithium metal anode, owing to the high thermal stability of both electrolyte [18] and cathode [29]. A relevant proof of the electrolyte suitability even under hazardous conditions is represented by the flammability test in reported in Fig. 1, carried out on the $\text{LiCF}_3\text{SO}_3\text{-LiNO}_3\text{-TEGDME}$ solution and, for comparison, on conventional carbonate-based electrolyte. Fig. 1a shows that flame exposure leads to fast ignition of the conventional $\text{LiPF}_6\text{-EC-DMC}$ electrolyte, followed by combustion up to almost full electrolyte consumption. Instead, the $\text{LiCF}_3\text{SO}_3\text{-LiNO}_3\text{-TEGDME}$ solution shows a remarkable stability and a complete absence of fire evolution, even towards prolonged flame exposure, as confirmed by Fig. 1b. The flash points of TEGDME, EC, and DMC may account for the observed enhanced stability of the proposed electrolyte with respect to standard carbonate-based solutions. Indeed, despite the flash point of TEGDME is 141 °C, which is slightly lower than that of EC (143 °C), the volatile DMC has a flash point as low as 16 °C. Therefore, 1:1 mixtures of EC and DMC, allowing proper ion conduction and commonly used in lithium-ion batteries, suffers by flammability issue mainly due to low flash point of DMC [43]. On the other hand, the $\text{LiCF}_3\text{SO}_3\text{-LiNO}_3\text{-TEGDME}$ solution is stable upon flame exposure by the experimental setup adopted in this work, as shown by Fig. 1, due to the relatively high flash point of TEGDME. Despite the non-flammability of the electrolyte in its pristine state, i.e., prior to cell assembly, possible formation of new side species during cycling that may alter the flammability of the

whole system, i.e., the battery composed of electrodes, electrolytes as well as decomposition products. The evaluation of such as complex system requires *ad hoc* extended study, including cell nailing and heating tests, as well as calorimetric, thermo-gravimetric and chemical detection techniques, e.g. as mass spectroscopy, upon cell operation such as that reported in literature for polymer cell [44]. This study exceeds the aim of the present work; however, we may reasonably expect the non-flammability of the pristine glyme-based electrolyte (Fig. 1b) to remarkably increase the safety level of the cell with respect to the flammable carbonate-based electrolyte reported in Fig. 1a.

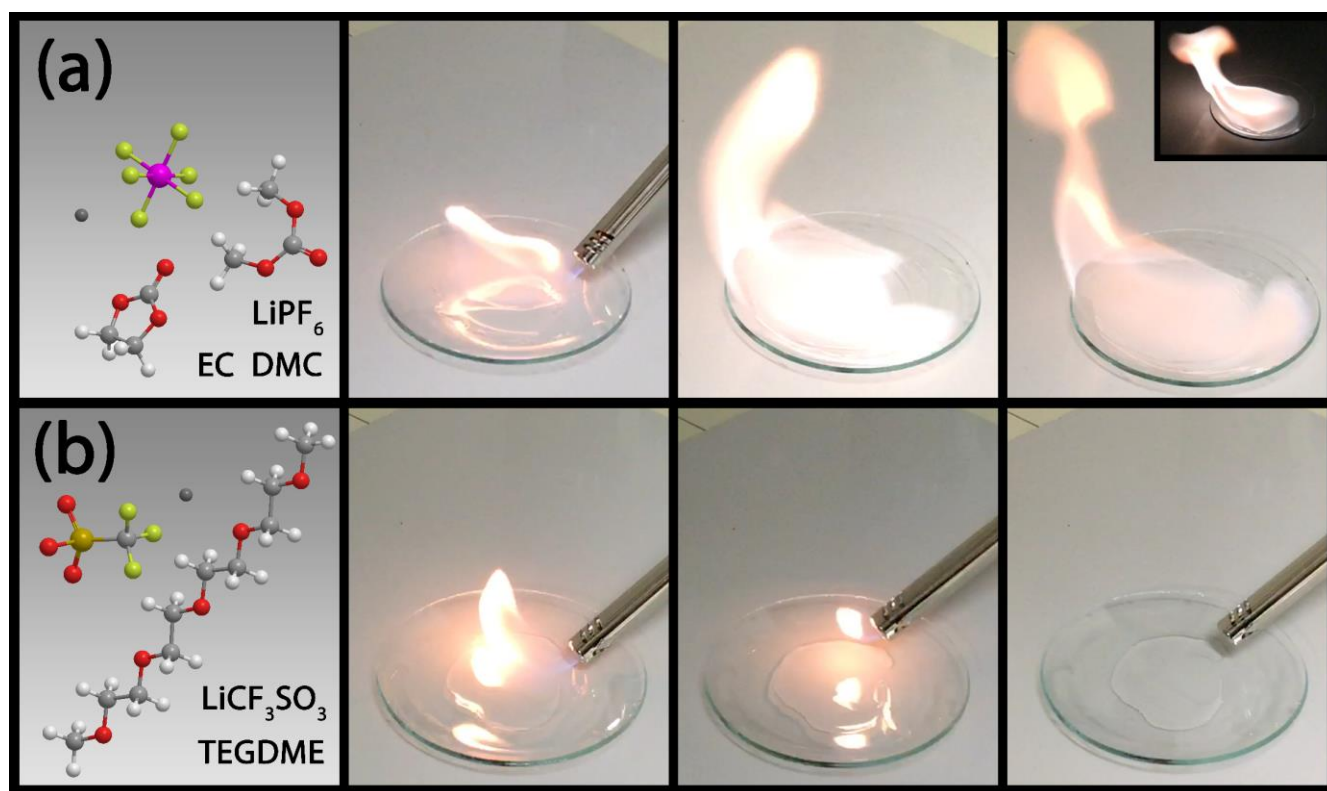


Figure 1. Flammability tests carried out on (a, top panels) conventional 1 M LiPF_6 in EC:DMC 1:1 w/w and (b, bottom panels) 1 mol kg^{-1} LiCF_3SO_3 , 1 mol kg^{-1} LiNO_3 in TEGDME.

LiFePO_4 and $\text{LiMn}_{0.5}\text{Fe}_{0.5}\text{PO}_4$ cathodes have been prepared by a simple solvothermal synthesis optimized in our laboratory, which leads to crystalline $\text{LiFe}_{1-a}\text{Mn}_a\text{PO}_4$ powders able to operate reversibly in lithium and lithium-ion cells [29,42]. Further careful characterization of the LiFePO_4 (Fig. 2a-c) and $\text{LiMn}_{0.5}\text{Fe}_{0.5}\text{PO}_4$ (Fig. 2d-f) materials has been carried out herein by SEM (panels a, d), SEM-EDS

(panels b, e), and TEM (panels c, f) considering the expected influence of sample morphology in controlling the electrochemical behavior of the electrode in glyme-based lithium cell. Fig. 2a, b reveals that the LiFePO_4 sample is homogeneously formed by sub-micrometric platelet-like particles, having uniform distribution of Fe and P in the 1:1 atomic ratio. The LiFePO_4 particles have elongated shape with maximum size of about 500 nm, as further shown by TEM (Fig. 2c). The $\text{LiMn}_{0.5}\text{Fe}_{0.5}\text{PO}_4$ material has comparable morphology, characterized by diamond-shaped platelets with maximum size of about 500 nm (see SEM of Fig. 2d and TEM of Fig. 2f). The EDS analysis reveals homogeneous distribution of Mn, Fe, and P over the $\text{LiMn}_{0.5}\text{Fe}_{0.5}\text{PO}_4$ grains, and quantification confirms sample stoichiometry (see corresponding EDS spectrum of Fig. S1 in the Supplementary Information). The particle size shown in Fig. 2 is considered suitable both for allowing a fast Li^+ transport through the one-dimensional olivine channels, and for limiting the decomposition of LiCF_3SO_3 -TEGDME-based solution during cell operation. Indeed, particle size reduction down to few tens of nanometers significantly enhances the electrochemical performances of $\text{LiFe}_{1-a}\text{Mn}_a\text{PO}_4$ cathodes, particularly at the higher Mn contents [31,41,45], however it contemporary favors electrolyte decomposition, interfacial resistance increase, and cell failure due to the deterioration of the electrode/electrolyte interface [40,41]. This aspect appears particularly relevant in view of the narrow oxidative stability windows of TEGDME– LiCF_3SO_3 solution (i.e., 4.5 V vs. Li^+/Li) [18] with respect to conventional LiPF_6 -carbonate electrolytes (above 4.7 V vs. Li^+/Li) [46]. Therefore, we have selected these particular cathode materials, characterized by sub-micrometric particles, for study in LiCF_3SO_3 - LiNO_3 -TEGDME electrolyte. As shown below, the cathode powders demonstrate suitable performances in the new electrolyte formulation without requiring further synthesis optimization.

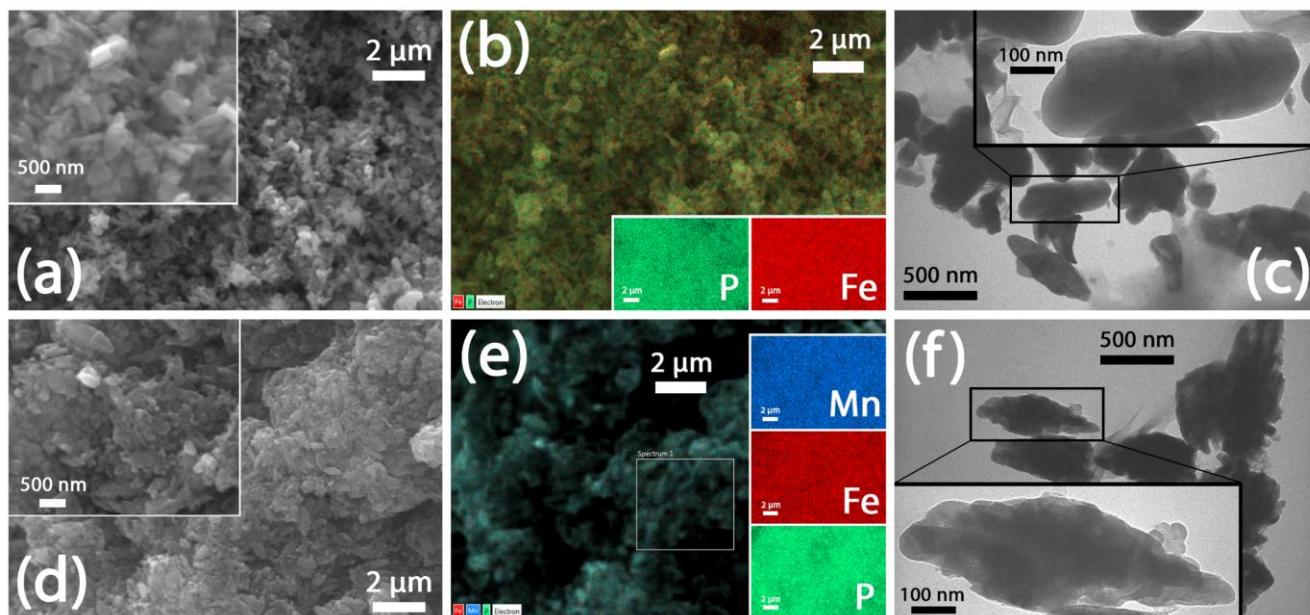


Figure 2. Electron microscopy analyses of (**top, a–c**) LiFePO_4 and (**bottom, d–f**) $\text{LiMn}_{0.5}\text{Fe}_{0.5}\text{PO}_4$ in terms of: (**a, d**) SEM images (magnification in **inset**); (**b, e**) SEM-EDS maps of (**blue**) Mn, (**red**) Fe, and (**green**) P over the sample powders (overlapped maps in the **main panel**; single maps in **inset**); (**c, f**) TEM images (magnification in **inset**).

Despite the relatively low dielectric constant of TEGDME and the large size of the LiCF_3SO_3 anion, we have demonstrated in our previous study that the combination of TEGDME and LiCF_3SO_3 leads to an electrolyte characterized by a conductivity ranging from $10^{-3} \text{ S cm}^{-1}$ at room temperature to a value exceeding $10^{-4} \text{ S cm}^{-1}$ at a temperature as low as -10°C [47]. These conductivity values, slightly lower than those expected for carbonate based electrolytes [48–50], are considered suitable for lithium cell application; however, they might partially limit the rate capability of the cell using LiFePO_4 at the lower temperatures. Furthermore, the TEGDME– LiCF_3SO_3 electrolyte has been herein added by LiNO_3 as film forming agent that allows a further stabilization of the SEI at the electrodes surface, as reported in a previous paper demonstrating the possible use in lithium cell with LiFePO_4 cathode of the electrolyte solution formed by dissolving LiCF_3SO_3 and LiNO_3 salts in high molecular weight glyme, i.e., polyethylene glycol dimethyl ether (PEG500DME) [27]. Electrochemical activation procedure has been proposed to form suitable electrode/electrolyte interface by LiNO_3 reaction. Accordingly, the cycling

tests herein reported have been carried out after performing 3 activation cycles reported in Fig. S2 in the Supplementary Information (see the experimental section for further details). The PEG500DME-based formulation proposed by the above mentioned paper [27] advantageously revealed low vapor pressure and high stability up to 400 °C, thus suggesting suitability for application at the higher temperatures; indeed, the electrolyte has shown lower ionic conductivity values at room temperature ($4 \times 10^{-4} \text{ S cm}^{-1}$) with respect to short-chain glyme (about $10^{-3} \text{ S cm}^{-1}$) and freezing point at 5 °C [18]. The $\text{LiCF}_3\text{SO}_3\text{-LiNO}_3\text{-PEG500DME}$ electrolyte allowed proper room temperature galvanostatic cycling of a Li/LiFePO_4 cell at C/5 rate ($1\text{C} = 170 \text{ mAh g}^{-1}$) [27]. On the other and, the TEGDME-based electrolyte herein proposed has thermal stability ranging from $-49 \text{ }^\circ\text{C}$ to $200 \text{ }^\circ\text{C}$ and ionic conductivity of about $1 \times 10^{-3} \text{ S cm}^{-1}$ at room temperature [18]; therefore, it is expected to ensure suitable performances in Li/LiFePO_4 cell at higher current rates and lower temperatures than PEG500DME. The high-rate performances have been herein demonstrated up to 2C rate ($1\text{C} = 170 \text{ mAh g}^{-1}$) for Li/LiFePO_4 and $\text{Li/LiMn}_{0.5}\text{Fe}_{0.5}\text{PO}_4$ cells, as following reported. Rate capability of the $\text{Li/LiCF}_3\text{SO}_3\text{-LiNO}_3\text{-TEGDME/LiFePO}_4$ cell has been evaluated by galvanostatic cycling at several current rates, as shown in Fig. 3. The voltage profiles (Fig. 3a) reveal plateaus centered at about 3.45 V, which indicate reversible two-phase reaction of LiFePO_4 [30]. The cell exhibits flat voltage profiles and low polarization (about 0.05 V) at slow rates; as expected, the rise of C-rate to 2C ($1\text{C} = 170 \text{ mA g}^{-1}$) produces slope of the voltage profile, polarization increase, and lower capacity. Indeed, the cell delivers reversible capacity of 152, 150, 145, 138, 125, and 112 mAh g^{-1} at C/10, C/5, C/3, C/2, 1C, and 2C ($1\text{C} = 170 \text{ mA g}^{-1}$), respectively (see Fig. 3b). These results demonstrate the full suitability of the $\text{LiCF}_3\text{SO}_3\text{-LiNO}_3\text{-TEGDME}$ electrolyte in lithium cells that use LiFePO_4 cathode. This cathode has been widely investigated over the last few years, leading to its current commercial use in cells [51]. In particular, recent literature works [52–55] reported LiFePO_4 powders prepared by solvothermal pathways characterized by excellent electrochemical performances in standard carbonate-based electrolyte. Hence, we compared the cycling results of lithium cells using $\text{LiCF}_3\text{SO}_3\text{-}$

LiNO₃-TEGDME and a common carbonate-based electrolyte, with the LiFePO₄ sample synthesized in our laboratory [29,42] (Fig. S3 in the Supplementary Information). In particular, Fig. S3 in the Supplementary Information shows the galvanostatic cycling performances at C/3 rate (1C = 170 mAh g⁻¹) of LiFePO₄ in 1 M LiPF₆ EC:DMC 1:1 w/w standard electrolyte and in the new LiCF₃SO₃-LiNO₃-TEGDME formulation. The cell using standard carbonate-based electrolyte delivers reversible capacity of 114 mAh g⁻¹ at the 1st cycle, which increases to 121 mAh g⁻¹ after 10 cycles due to cathode structural reorganization already observed for similar olivine materials [29,38,42]; at the 30th cycle the capacity slight decreases to 117 mAh g⁻¹, i.e., 103 % and 97 % with respect to the 1st cycle and 10th cycle values, respectively. The glyme-based electrolyte ensures capacity of 124 mAh g⁻¹ and 126 mAh g⁻¹ at the 1st and 10th cycles, respectively; at the 30th cycle the capacity is 120 mAh g⁻¹, i.e., 97 % and 95 % with respect to the 1st cycle and 10th cycle values, respectively. Therefore, these results further demonstrate the applicability of TEGDME-based electrolyte in Li/LiFePO₄ cell: indeed, the cells employing TEGDME-based electrolyte exhibit comparable electrochemical behavior with higher capacity with respect to the conventional carbonate-based electrolyte. This observation has been confirmed by several tests in lithium cell. However, the cell using glyme suffers more capacity fading, which may be ascribed to not fully optimized LiFePO₄/electrolyte interface. This issue could be addressed by further tuning of the electrochemical activation procedure, which is expected to improve the SEI films attributed to nitrate reaction [27]. It is noteworthy that the first attempts to employ LiCF₃SO₃-glyme solutions in lithium cells with insertion cathodes revealed very poor electrochemical stability, which has been remarkably improved by LiNO₃ addition, as shown by Fig. S3. The figure also reveals the beneficial effect on the cell performances of C-cloth support with respect to standard Al foil as well. In particular, we have compared the cycling behavior at C/3 rate (1C = 170 mAh g⁻¹) of two Li/ LiCF₃SO₃-LiNO₃-TEGDME/LiFePO₄ cells only differing in the current collector.

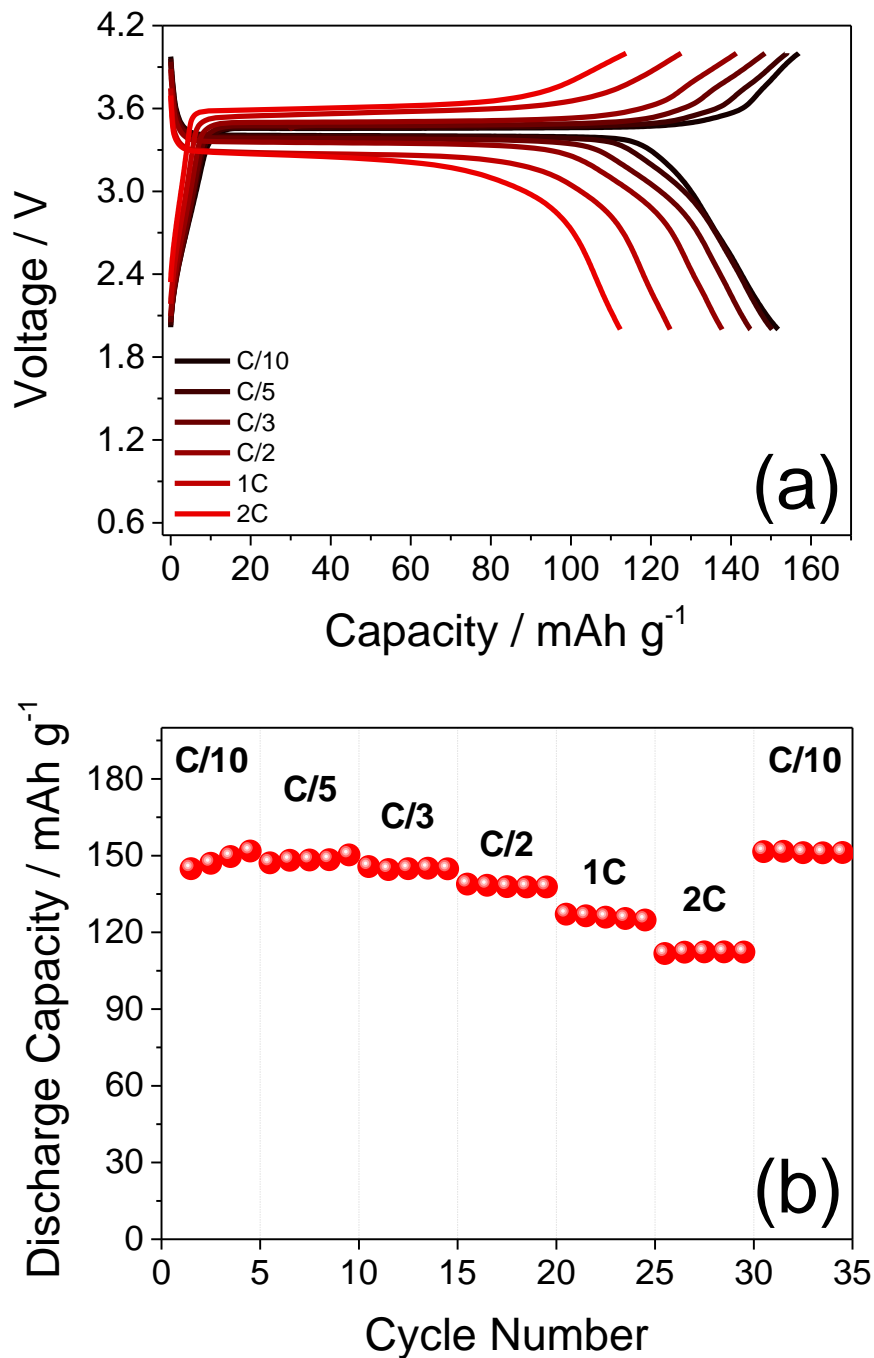


Figure 3. Rate capability test of the Li/LiCF₃SO₃-LiNO₃-TEGDME/LiFePO₄ cell in terms of (a) voltage profiles and (b) cycling behavior, performed by galvanostatic cycling at C/10, C/5, C/3, C/2, 1C, and 2C rates (1C = 170 mAh g⁻¹) within the 2 – 4 V voltage range; test performed after electrochemical activation [27] of the cell (see the experimental section and Fig. S2 in the Supplementary Information); room temperature (25 °C).

Fig. S3 clearly shows a capacity improvement due to C-cloth from 126 mAh g^{-1} to 139 mAh g^{-1} , which is likely related to the higher surface area of the electrode support with respect to Al disk. This particular current collector morphology enhances the electric contact between olivine particles and current collector and increases the effective cathode/electrolyte interface (see schematic representation of the electrodes morphology in Fig S4). Furthermore, additional polarization ascribed to the Li/electrolyte interface may be possibly excluded by the cycling test of the lithium anode in symmetrical Li/ LiCF_3SO_3 (- LiNO_3)-TEGDME/Li cell reported the supplementary information section, Fig. S5.

Fig. 4 shows the galvanostatic cycling performances of the Li/ LiCF_3SO_3 - LiNO_3 -TEGDME/ LiFePO_4 cell at C/3 (panels a, b) and 2C rates (panels c, d; $1\text{C} = 170 \text{ mA g}^{-1}$) upon 100 cycles. The Li/ LiFePO_4 cell cycled at C/3 rate exhibits flat plateaus with limited polarization, which slight evolve throughout cycling (see Fig. 4). This phenomenon may be related to irreversible processes leading to coulombic efficiency of 97%, and it is reflected into capacity fading from about 140 mAh g^{-1} at the first cycles to 110 mAh g^{-1} at the 100th cycle (see Fig. 4b). Low coulombic efficiency values and capacity fading are likely attributed to a not fully optimized LiFePO_4 /electrolyte interface, as well as to the reactive lithium metal interface and the adopted T-cell configuration, which is commonly used for short-time cycling. Indeed, previous reports on lithium-sulfur cells demonstrated that LiNO_3 addition to glyme-based electrolytes leads to formation of a stable lithium/electrolyte interface [12–14,56]. This approach may also be useful for allowing reversible operation of lithium cells using insertion cathodes, which form very poor electrode/electrolyte interface with pristine LiCF_3SO_3 -glyme solution [27]. Nevertheless, the results of Fig. 4 suggest further work aimed at fully understanding and possibly improving the LiFePO_4 /electrolyte as well as the lithium/electrolyte interfaces. Accordingly, deep characterization of the electrochemical activation process, currently in progress in our laboratory, might lead to electrode/electrolyte interface enhancement for prolonged cycling in coin-cell configuration; however, this is beyond the scope of our paper, which indeed demonstrates reversible operation at of Li/ LiFePO_4

cells using LiCF_3SO_3 -TEGDME electrolyte. Higher efficiency values, i.e., of about 99%, are obtained by rising the C-rate to 2C, thus allowing enhanced cycling stability with reversible capacity of 100 mAh g^{-1} (Fig. 4d) and expected cell polarization increases (Fig. 4c). The improvement of stability at high C-rate is likely related to decreased magnitude of parasitic reactions at the electrode/electrolyte interface.

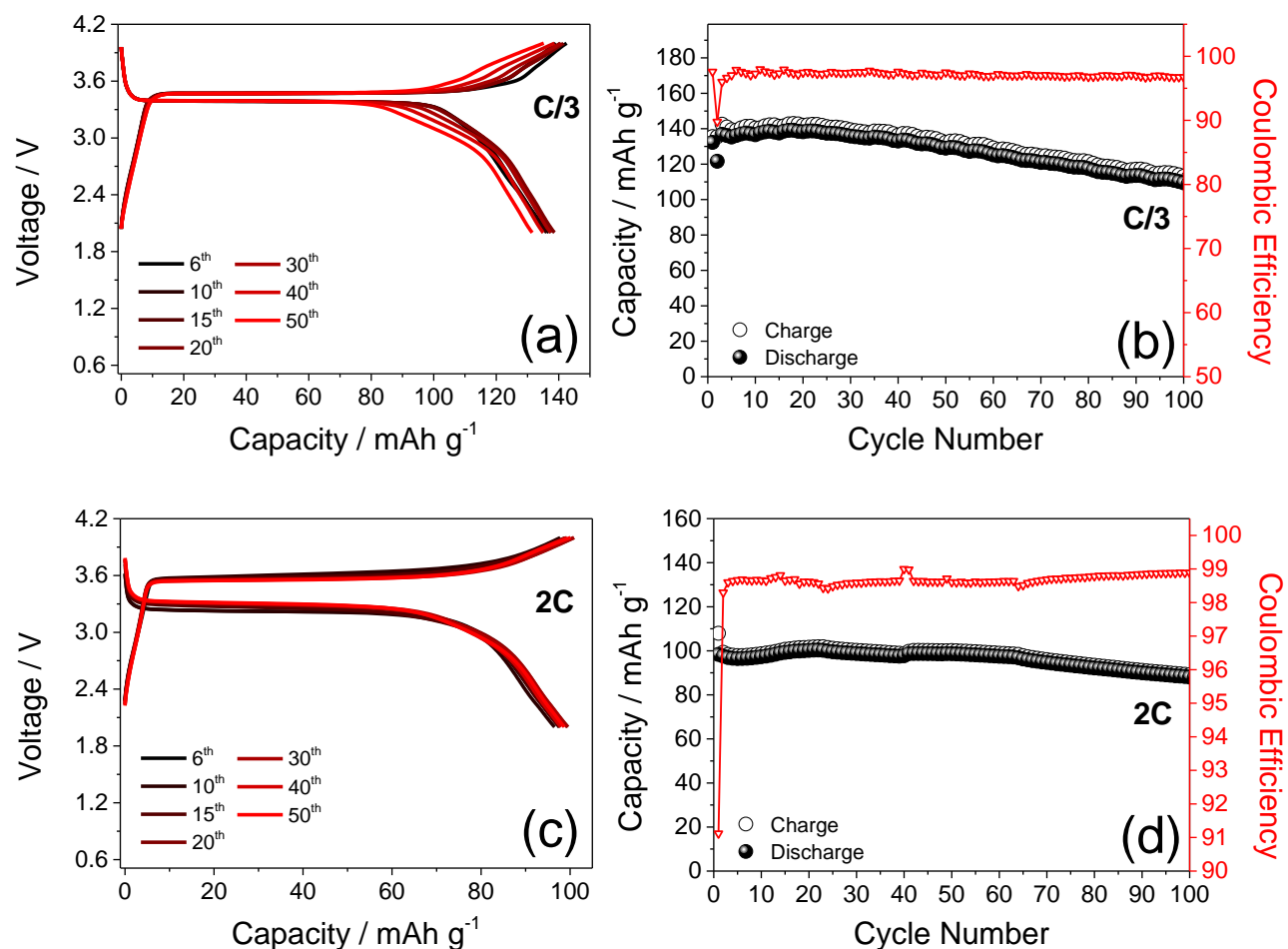


Figure 4. Galvanostatic tests of $\text{Li/LiCF}_3\text{SO}_3\text{-LiNO}_3\text{-TEGDME/LiFePO}_4$ cells in terms of (a, c) voltage profiles and (b, d) cycling behavior within the 2 – 4 V voltage range at two C-rates: (a, b) C/3, and (c, d) 2C rates ($1\text{C} = 170 \text{ mAh g}^{-1}$); test performed after electrochemical activation [27] of the cell (see the experimental section and Fig. S2 in the Supplementary Information); room temperature ($25 \text{ }^\circ\text{C}$).

Fig. 5 reports a rate capability test of the $\text{LiMn}_{0.5}\text{Fe}_{0.5}\text{PO}_4$ cathode in the $\text{LiCF}_3\text{SO}_3\text{-LiNO}_3\text{-TEGDME}$ electrolyte. The voltage profiles (Fig. 5a) clearly evidence the electrochemical fingerprints of the $\text{Fe}^{3+}/\text{Fe}^{2+}$ [30] and $\text{Mn}^{3+}/\text{Mn}^{2+}$ [31] couples at the various rates. Fig. 5b shows reversible capacity

values of 166, 148, 130, 120, 99, and 73 mAh g⁻¹ at C/10, C/5, C/3, C/2, 1C, and 2C (1C = 170 mA g⁻¹), respectively.

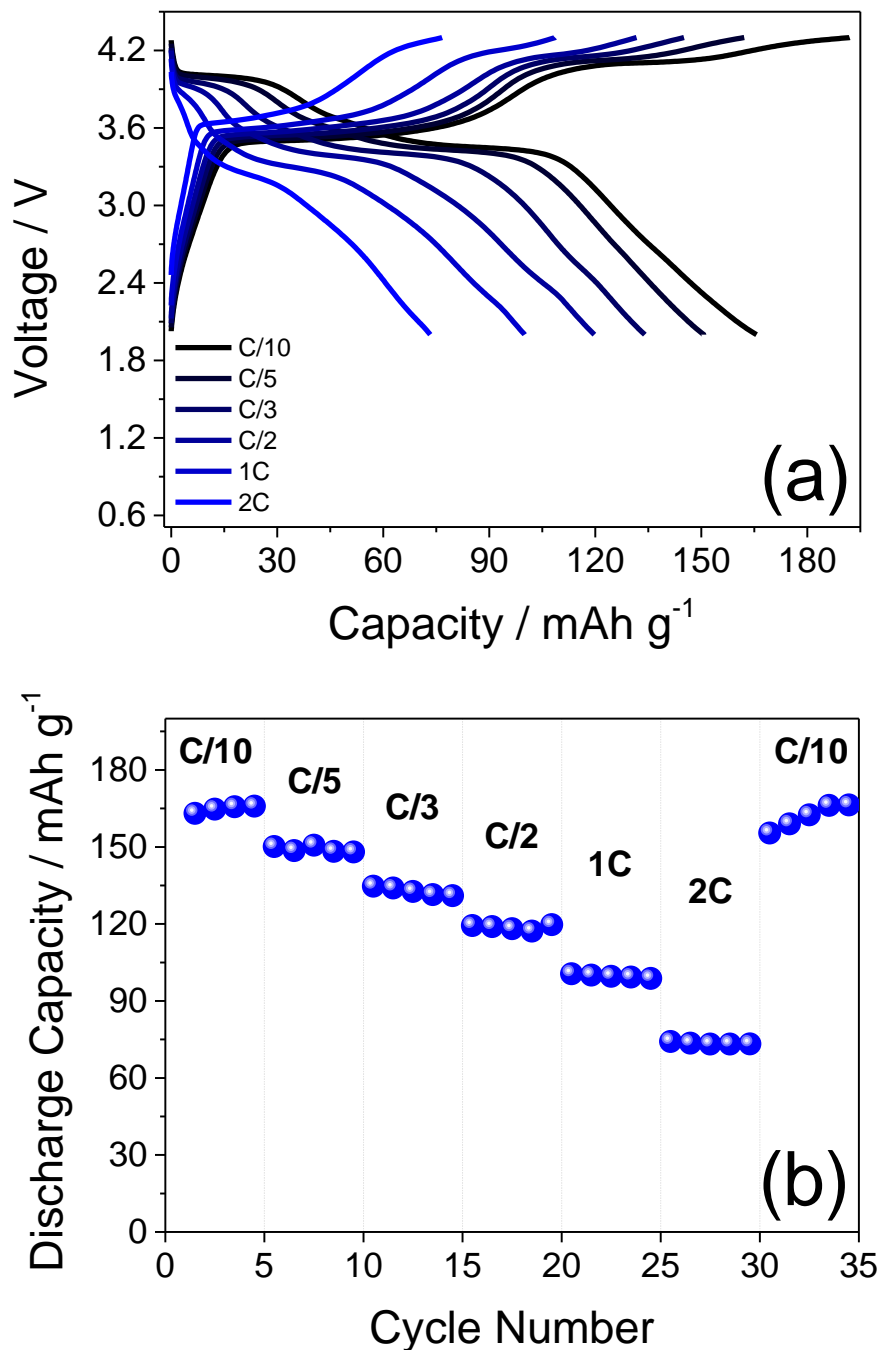


Figure 5. Rate capability test of the Li/LiCF₃SO₃-LiNO₃-TEGDME/LiMn_{0.5}Fe_{0.5}PO₄ cell in terms of (a) voltage profiles and (b) cycling behavior, performed by galvanostatic cycling at C/10, C/5, C/3, C/2, 1C, and 2C rates (1C = 170 mAh g⁻¹) within the 2 – 4.3 V voltage range; test performed after electrochemical

activation [27] of the cell (see the experimental section and Fig. S2 in the Supplementary Information); room temperature (25 °C).

It is noteworthy that the Li/LiCF₃SO₃-LiNO₃-TEGDME/LiMn_{0.5}Fe_{0.5}PO₄ cell exhibits lower performance at high rates with respect to the cell using LiFePO₄ (compare Fig. 3 and Fig. 5), owing to the well-known kinetic hindrance to Li⁺ insertion/deinsertion of LiFe_{1- α} Mn _{α} PO₄ phases [42]. The rate capability test of the Li/LiCF₃SO₃-LiNO₃-TEGDME/LiMn_{0.5}Fe_{0.5}PO₄ cell suggests the system particularly suitable for application at the lower currents. Therefore, we have studied the galvanostatic performances over 100 cycles using C/5 rate (1C = 170 mA g⁻¹).

Fig. 6 demonstrates reversible operation of the Li/LiCF₃SO₃-LiNO₃-TEGDME/LiMn_{0.5}Fe_{0.5}PO₄ cell, with relatively stable voltage profile upon cycling (Fig. 6a) and reversible capacity of about 125 mAh g⁻¹. However, the cell exhibits coulombic efficiency values of about 95% and capacity fading to 94 mAh g⁻¹ at the 100th cycle, i.e., a cycling performance less remarkable than that one of the Li/LiCF₃SO₃-LiNO₃-TEGDME/LiFePO₄ cell. As already reported in Fig. 4 discussion, we partially attribute this drawback to not fully optimized cathode/electrolyte interface. Furthermore, the higher working voltage of LiMn_{0.5}Fe_{0.5}PO₄ with respect to LiFePO₄ may account for the observed cell performance. Indeed, the higher voltage cutoff used for the Li/LiCF₃SO₃-LiNO₃-TEGDME/LiMn_{0.5}Fe_{0.5}PO₄ cell allows proper operation at the Mn³⁺/Mn²⁺ potential, but contemporary induces a concomitant electrolyte decomposition. Accordingly, a previous work revealed that the electrolyte undergoes oxidation at about 4.5 V vs. Li⁺/Li [18], which is close to the voltage cutoff used herein. In addition, comparison of Fig. 5 and Fig. 6 reveals higher capacity values at the higher currents with respect to the galvanostatic cycling at single rate, similarly to the trend observed for the lithium cell using LiFePO₄ by comparing Fig. 3 and Fig. 4. Accordingly, further optimization of electrolyte composition and electrochemical activation procedure might address these issues.

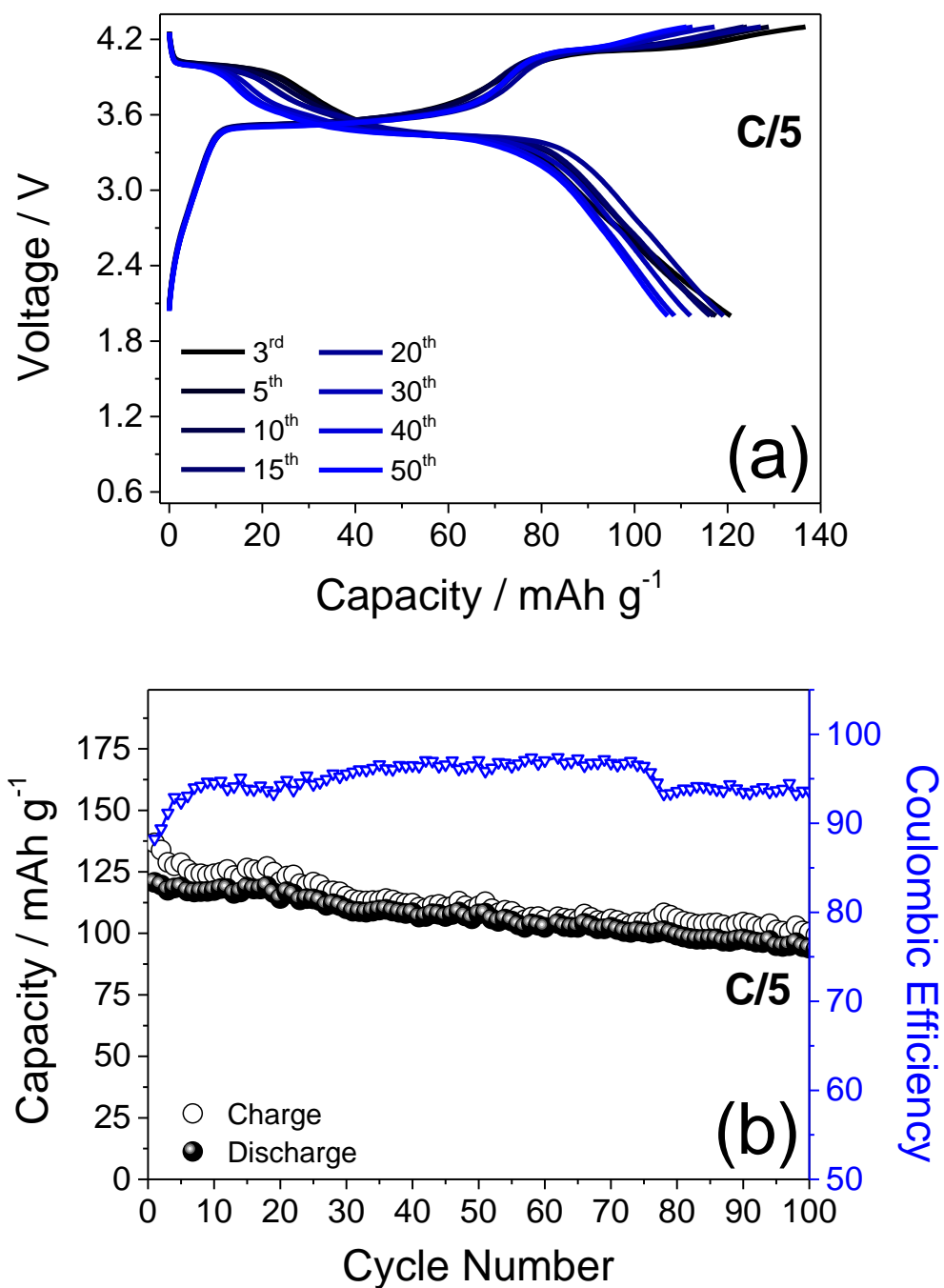


Figure 6. Galvanostatic cycling tests of Li/LiCF₃SO₃-LiNO₃-TEGDME/LiMn_{0.5}Fe_{0.5}PO₄ cells in terms of (a) voltage profiles and (b) cycling behavior at C/5 rate (1C = 170 mAh g⁻¹) within the 2 – 4.3 V voltage range; test performed after electrochemical activation [27] of the cell (see the experimental section and Fig. S2 in the Supplementary Information); temperature = 25 °C.

Conclusion

The present study revealed a possible strategy to employ high energy lithium metal in safe and high energy rechargeable batteries. LiFePO_4 and $\text{LiMn}_{0.5}\text{Fe}_{0.5}\text{PO}_4$ olivine cathodes were studied in lithium cells with a glyme-based electrolyte solution having composition $1 \text{ mol kg}^{-1} \text{ LiCF}_3\text{SO}_3$, $1 \text{ mol kg}^{-1} \text{ LiNO}_3$ in TEGDME. Flammability tests demonstrated the electrolyte stability under hazardous conditions, thus suggesting possible applicability in combination with lithium metal anode. Scanning and transmission electron microscopies, as well as X-ray energy dispersive analysis of the olivine powders, evidenced submicrometrical particles with homogenous atomic distribution. This morphology allowed proper operation of the lithium cell using TEGDME-based electrolyte, as demonstrated by galvanostatic cycling tests. In particular, $\text{Li/LiCF}_3\text{SO}_3\text{-LiNO}_3\text{-TEGDME/LiFePO}_4$ and $\text{Li/LiCF}_3\text{SO}_3\text{-LiNO}_3\text{-TEGDME/LiMn}_{0.5}\text{Fe}_{0.5}\text{PO}_4$ cells exhibit promising rate performances and stable cycling trends, thus actually suggesting the suitability of the proposed combination as promising energy storage systems.

Acknowledgements

The work was performed within the collaboration project “Accordo di Collaborazione Quadro 2015” between the University of Ferrara (Department of Chemical and Pharmaceutical Sciences) and Sapienza University of Rome (Chemistry Department). The authors thank Daniela Palmeri (Electronic Microscopy Centre, Department of Chemical and Pharmaceutical Sciences, University of Ferrara) for performing SEM and TEM images.

References

- [1] L. Croguennec, M.R. Palacin, Recent achievements on inorganic electrode materials for lithium-ion batteries, *J. Am. Chem. Soc.* 137 (2015) 3140–3156. doi:10.1021/ja507828x.
- [2] K. Xu, Electrolytes and interphases in Li-ion batteries and beyond, *Chem. Rev.* 114 (2014) 11503–11618. doi:10.1021/cr500003w.
- [3] B. Scrosati, J. Garche, Lithium batteries: Status, prospects and future, *J. Power Sources.* 195 (2010) 2419–2430. doi:10.1016/j.jpowsour.2009.11.048.
- [4] W. Xu, J. Wang, F. Ding, X. Chen, E. Nasybulin, Y. Zhang, J.-G. Zhang, Lithium metal anodes for rechargeable batteries, *Energy Environ. Sci.* 7 (2014) 513–537. doi:10.1039/C3EE40795K.
- [5] P.G. Balakrishnan, R. Ramesh, T. Prem Kumar, Safety mechanisms in lithium-ion batteries, *J. Power Sources.* 155 (2006) 401–414. doi:10.1016/j.jpowsour.2005.12.002.
- [6] Q. Wang, P. Ping, X. Zhao, G. Chu, J. Sun, C. Chen, Thermal runaway caused fire and explosion of lithium ion battery, *J. Power Sources.* 208 (2012) 210–224. doi:10.1016/j.jpowsour.2012.02.038.
- [7] F. Croce, G.B. Appetecchi, L. Persi, B. Scrosati, Nanocomposite polymer electrolytes for lithium batteries, *Nature.* 394 (1998) 456–458. doi:10.1038/28818.
- [8] T. Yamada, S. Ito, R. Omoda, T. Watanabe, Y. Aihara, M. Agostini, U. Ulissi, J. Hassoun, B. Scrosati, All Solid-State Lithium-Sulfur Battery Using a Glass-Type P2S5-Li2S Electrolyte: Benefits on Anode Kinetics, *J. Electrochem. Soc.* 162 (2015) A646–A651. doi:10.1149/2.0441504jes.
- [9] S. Tobishima, H. Morimoto, M. Aoki, Y. Saito, T. Inose, T. Fukumoto, T. Kuryu, Glyme-based

- nonaqueous electrolytes for rechargeable lithium cells, *Electrochim. Acta.* 49 (2004) 979–987. doi:10.1016/j.electacta.2003.10.009.
- [10] D. Aurbach, E. Granot, The study of electrolyte solutions based on solvents from the “glyme” family (linear polyethers) for secondary Li battery systems, *Electrochim. Acta.* 42 (1997) 697–718. doi:10.1016/S0013-4686(96)00231-9.
- [11] Y. Choquette, Sulfamides and Glymes as Aprotic Solvents for Lithium Batteries, *J. Electrochem. Soc.* 145 (1998) 3500. doi:10.1149/1.1838834.
- [12] S. Xiong, K. Xie, Y. Diao, X. Hong, Properties of surface film on lithium anode with LiNO₃ as lithium salt in electrolyte solution for lithium-sulfur batteries, *Electrochim. Acta.* 83 (2012) 78–86. doi:10.1016/j.electacta.2012.07.118.
- [13] C. Barchasz, J.-C. Lepretre, S. Patoux, F. Alloin, Revisiting TEGDME/DIOX Binary Electrolytes for Lithium/Sulfur Batteries: Importance of Solvation Ability and Additives, *J. Electrochem. Soc.* 160 (2013) A430–A436. doi:10.1149/2.022303jes.
- [14] A. Rosenman, R. Elazari, G. Salitra, E. Markevich, D. Aurbach, A. Garsuch, The Effect of Interactions and Reduction Products of LiNO₃, the Anti-Shuttle Agent, in Li-S Battery Systems, *J. Electrochem. Soc.* 162 (2015) A470–A473. doi:10.1149/2.0861503jes.
- [15] A. Manthiram, Y. Fu, Y.-S. Su, Challenges and Prospects of Lithium–Sulfur Batteries, *Acc. Chem. Res.* 46 (2013) 1125–1134. doi:10.1021/ar300179v.
- [16] Y.X. Yin, S. Xin, Y.G. Guo, L.J. Wan, Lithium-sulfur batteries: Electrochemistry, materials, and prospects, *Angew. Chemie - Int. Ed.* 52 (2013) 13186–13200. doi:10.1002/anie.201304762.
- [17] J. Kim, D.J. Lee, H.G. Jung, Y.K. Sun, J. Hassoun, B. Scrosati, An advanced lithium-sulfur battery, *Adv. Funct. Mater.* 23 (2013) 1076–1080. doi:10.1002/adfm.201200689.

- [18] L. Carbone, M. Gobet, J. Peng, M. Devany, B. Scrosati, S. Greenbaum, J. Hassoun, Comparative study of Ether-based electrolytes for application in Lithium-Sulfur Battery, *ACS Appl. Mater. Interfaces*. (2015) 150609133700003. doi:10.1021/acsami.5b02160.
- [19] S.S. Zhang, Liquid electrolyte lithium/sulfur battery: Fundamental chemistry, problems, and solutions, *J. Power Sources*. 231 (2013) 153–162. doi:10.1016/j.jpowsour.2012.12.102.
- [20] C.O. Laoire, S. Mukerjee, E.J. Plichta, M.A. Hendrickson, K.M. Abraham, Rechargeable Lithium/TEGDME-LiPF₆O₂ Battery, *J. Electrochem. Soc.* 158 (2011) A302. doi:10.1149/1.3531981.
- [21] H.-G. Jung, J. Hassoun, J.-B. Park, Y.-K. Sun, B. Scrosati, An improved high-performance lithium–air battery, *Nat. Chem.* 4 (2012) 579–585. doi:10.1038/nchem.1376.
- [22] L. Grande, E. Paillard, J. Hassoun, J.-B. Park, Y.-J. Lee, Y.-K. Sun, S. Passerini, B. Scrosati, The Lithium/Air Battery: Still an Emerging System or a Practical Reality?, *Adv. Mater.* 27 (2015) 784–800. doi:10.1002/adma.201403064.
- [23] G.A. Elia, R. Bernhard, J. Hassoun, A lithium-ion oxygen battery using a polyethylene glyme electrolyte mixed with an ionic liquid, *RSC Adv.* 5 (2015) 21360–21365. doi:10.1039/C4RA17277A.
- [24] K.M. Abraham, Electrolyte-Directed Reactions of the Oxygen Electrode in Lithium-Air Batteries, *J. Electrochem. Soc.* 162 (2015) A3021–A3031. doi:10.1149/2.0041502jes.
- [25] D.J. Lee, J. Hassoun, S. Panero, Y.K. Sun, B. Scrosati, A tetraethylene glycol dimethylether-lithium bis(oxalate)borate (TEGDME-LiBOB) electrolyte for advanced lithium ion batteries, *Electrochem. Commun.* 14 (2012) 43–46. doi:10.1016/j.elecom.2011.10.027.
- [26] R. Bernhard, A. Latini, S. Panero, B. Scrosati, J. Hassoun, Poly(ethylenglycol)dimethylether–

- lithium bis(trifluoromethanesulfonyl)imide, PEG500DME–LiTFSI, as high viscosity electrolyte for lithium ion batteries, *J. Power Sources*. 226 (2013) 329–333.
doi:10.1016/j.jpowsour.2012.10.059.
- [27] L. Carbone, M. Gobet, J. Peng, M. Devany, B. Scrosati, S. Greenbaum, J. Hassoun, Polyethylene glycol dimethyl ether (PEGDME)-based electrolyte for lithium metal battery, *J. Power Sources*. 299 (2015) 460–464. doi:10.1016/j.jpowsour.2015.08.090.
- [28] A. Yamada, S.C. Chung, K. Hinokuma, Optimized LiFePO₄ for Lithium Battery Cathodes, *J. Electrochem. Soc.* 148 (2001) A224. doi:10.1149/1.1348257.
- [29] D. Di Lecce, C. Fasciani, B. Scrosati, J. Hassoun, A Gel–Polymer Sn–C/LiMn_{0.5}Fe_{0.5}PO₄ Battery Using a Fluorine-Free Salt, *ACS Appl. Mater. Interfaces*. 7 (2015) 21198–21207.
doi:10.1021/acsami.5b05179.
- [30] A.K. Padhi, K.S. Nanjundaswamy, J.B. Goodenough, Phospho-olivines as Positive-Electrode Materials for Rechargeable Lithium Batteries, *J. Electrochem. Soc.* 144 (1997) 1188–1194.
- [31] V. Aravindan, J. Gnanaraj, Y.-S. Lee, S. Madhavi, LiMnPO₄ – A next generation cathode material for lithium-ion batteries, *J. Mater. Chem. A*. 1 (2013) 3518–3539.
doi:10.1039/c2ta01393b.
- [32] J. Chen, M.J. Vacchio, S. Wang, N. Chernova, P.Y. Zavalij, M.S. Whittingham, The hydrothermal synthesis and characterization of olivines and related compounds for electrochemical applications, *Solid State Ionics*. 178 (2008) 1676–1693.
doi:10.1016/j.ssi.2007.10.015.
- [33] a. V. Murugan, T. Muraliganth, a. Manthiram, Comparison of microwave assisted solvothermal and hydrothermal syntheses of LiFePO₄/C nanocomposite cathodes for lithium ion batteries, *J.*

Phys. Chem. C. 112 (2008) 14665–14671. doi:10.1021/jp8053058.

- [34] Y.K. Sun, S.M. Oh, H.K. Park, B. Scrosati, Micrometer-sized, nanoporous, high-volumetric-capacity $\text{LiMn}_{0.85}\text{Fe}_{0.15}\text{PO}_4$ cathode material for rechargeable lithium-ion batteries, *Adv. Mater.* 23 (2011) 5050–5054. doi:10.1002/adma.201102497.
- [35] S.-M. Oh, S.-T. Myung, J.B. Park, B. Scrosati, K. Amine, Y.-K. Sun, Double-structured $\text{LiMn}_{0.85}\text{Fe}_{0.15}\text{PO}_4$ coordinated with LiFePO_4 for rechargeable lithium batteries., *Angew. Chemie Int. Ed.* 51 (2012) 1853–6. doi:10.1002/ange.201107394.
- [36] K. Saravanan, V. Ramar, P. Balaya, J.J. Vittal, $\text{Li}(\text{Mn}_x\text{Fe}_{1-x})\text{PO}_4/\text{C}$ ($x = 0.5, 0.75$ and 1) nanoplates for lithium storage application, *J. Mater. Chem.* 21 (2011) 14925. doi:10.1039/c1jm11541c.
- [37] Z. Lu, H. Chen, R. Robert, B.Y.X. Zhu, J. Deng, L. Wu, C.Y. Chung, C.P. Grey, Citric Acid-and Ammonium-Mediated Morphological Transformations of Olivine LiFePO_4 Particles, *Chem. Mater.* 23 (2011) 2848–2859.
- [38] D. Di Lecce, R. Brescia, A. Scarpellini, M. Prato, J. Hassoun, A High Voltage Olivine Cathode for Application in Lithium-Ion Batteries, *ChemSusChem.* 9 (2016) 223–230. doi:10.1002/cssc.201501330.
- [39] S. Yang, M. Hu, L. Xi, R. Ma, Y. Dong, C.Y. Chung, Solvothermal Synthesis of Monodisperse LiFePO_4 Micro Hollow Spheres as High Performance Cathode Material for Lithium Ion Batteries, (2013).
- [40] J.M. Zheng, X.B. Wu, Y. Yang, A comparison of preparation method on the electrochemical performance of cathode material $\text{Li}[\text{Li}_{0.2}\text{Mn}_{0.54}\text{Ni}_{0.13}\text{Co}_{0.13}]\text{O}_2$ for lithium ion battery, *Electrochim. Acta.* 56 (2011) 3071–3078. doi:10.1016/j.electacta.2010.12.049.

- [41] K. Zaghib, A. Guerfi, P. Hovington, A. Vijn, M. Trudeau, A. Mauger, J.B. Goodenough, C.M. Julien, Review and analysis of nanostructured olivine-based lithium rechargeable batteries: Status and trends, *J. Power Sources*. 232 (2013) 357–369. doi:10.1016/j.jpowsour.2012.12.095.
- [42] D. Di Lecce, J. Hassoun, Lithium Transport Properties in $\text{LiMn}_{1-\alpha}\text{Fe}_{\alpha}\text{PO}_4$ Olivine Cathodes, *J. Phys. Chem. C*. 119 (2015) 20855–20863. doi:10.1021/acs.jpcc.5b06727.
- [43] C. Arbizzani, G. Gabrielli, M. Mastragostino, Thermal stability and flammability of electrolytes for lithium-ion batteries, *J. Power Sources*. 196 (2011) 4801–4805. doi:10.1016/j.jpowsour.2011.01.068.
- [44] J. Hassoun, P. Reale, S. Panero, B. Scrosati, M. Wachtler, M. Fleischhammer, M. Kasper, M. Wohlfahrt-Mehrens, Determination of the safety level of an advanced lithium ion battery having a nanostructured Sn-C anode, a high voltage $\text{LiNi}_0.5\text{Mn}_{1.5}\text{O}_4$ cathode, and a polyvinylidene fluoride-based gel electrolyte, *Electrochim. Acta*. 55 (2010) 4194–4200. doi:10.1016/j.electacta.2010.02.063.
- [45] K.T. Lee, J. Cho, Roles of nanosize in lithium reactive nanomaterials for lithium ion batteries, *Nano Today*. 6 (2011) 28–41. doi:10.1016/j.nantod.2010.11.002.
- [46] K. Xu, Nonaqueous liquid electrolytes for lithium-based rechargeable batteries, *Chem. Rev.* 104 (2004) 4303–4417. doi:10.1021/cr030203g.
- [47] J. Hassoun, J. Kim, D.J. Lee, H.G. Jung, S.M. Lee, Y.K. Sun, B. Scrosati, A contribution to the progress of high energy batteries: A metal-free, lithium-ion, silicon-sulfur battery, *J. Power Sources*. 202 (2012) 308–313. doi:10.1016/j.jpowsour.2011.11.060.
- [48] M.S. Ding, K. Xu, S.S. Zhang, K. Amine, G.L. Henriksen, T.R. Jow, Change of Conductivity with Salt Content, Solvent Composition, and Temperature for Electrolytes of LiPF_6 in Ethylene

Carbonate-Ethyl Methyl Carbonate, *J. Electrochem. Soc.* 148 (2001) A1196.

doi:10.1149/1.1403730.

- [49] L.O. Valoén, J.N. Reimers, Transport Properties of LiPF₆-Based Li-Ion Battery Electrolytes, *J. Electrochem. Soc.* 152 (2005) A882. doi:10.1149/1.1872737.
- [50] S. Zugmann, M. Fleischmann, M. Amereller, R.M. Gschwind, H.D. Wiemhöfer, H.J. Gores, Measurement of transference numbers for lithium ion electrolytes via four different methods, a comparative study, *Electrochim. Acta.* 56 (2011) 3926–3933.
doi:10.1016/j.electacta.2011.02.025.
- [51] J. Wang, X. Sun, Understanding and recent development of carbon coating on LiFePO₄ cathode materials for lithium-ion batteries, *Energy Environ. Sci.* 5 (2012) 5163.
doi:10.1039/c1ee01263k.
- [52] J. Zhu, J. Fiore, D. Li, N.M. Kinsinger, Q. Wang, E. DiMasi, J. Guo, D. Kisailus, Solvothermal Synthesis, Development, and Performance of LiFePO₄ Nanostructures, *Cryst. Growth Des.* 13 (2013) 4659–4666. doi:10.1021/cg4013312.
- [53] S. Yang, X. Zhou, J. Zhang, Z. Liu, Morphology-controlled solvothermal synthesis of LiFePO₄ as a cathode material for lithium-ion batteries, *J. Mater. Chem.* 20 (2010) 8086.
doi:10.1039/c0jm01346c.
- [54] X. Rui, X. Zhao, Z. Lu, H. Tan, D. Sim, H.H. Hng, R. Yazami, T.M. Lim, Q. Yan, Olivine-type nanosheets for lithium ion battery cathodes, *ACS Nano.* 7 (2013) 5637–5646.
doi:10.1021/nn4022263.
- [55] Y. Wang, B. Zhu, Y. Wang, F. Wang, Solvothermal synthesis of LiFePO₄ nanorods as high-performance cathode materials for lithium ion batteries, *Ceram. Int.* 42 (2016) 10297–10303.

doi:10.1016/j.ceramint.2016.03.165.

- [56] M. Agostini, D.-J. Lee, B. Scrosati, Y.K. Sun, J. Hassoun, Characteristics of Li₂S₈-tetraglyme catholyte in a semi-liquid lithium–sulfur battery, *J. Power Sources*. 265 (2014) 14–19.

doi:10.1016/j.jpowsour.2014.04.074.